CARMA Memorandum Series #19

Version 1 CARMA Configurations for Cedar Flat

Tamara T. Helfer and Melvyn C. H. Wright
Radio Astronomy Lab, UCB

February 4, 2004

ABSTRACT

We present a set of six CARMA configurations for the Cedar Flat site, using six 10.4m OVRO antennas and nine 6.1m BIMA antennas. The configurations include a compact F array, which is designed to have good *uv* coverage at the shortest allowed spacings without sacrificing beam quality. The E, D, C, and A arrays have roughly constant scale resolution factors of ∼2–2.5 between adjacent arrays. An alternate long-baseline B array is included that is an elongated maximal array using the site constraint that all antennas lie east of Rte 168. All together, 65 stations are needed to populate the six arrays, if no central concrete slab is used.

Change Record

Revision	Date	Author	Sections/Pages Affected
	Remarks		
1.0	2003-Apr-11	T.T. Helfer	
	Original version, submitted to CARMA Memo series on 2004-Feb-04.		

1. Introduction

In this document, we present a set of six CARMA configurations for the Cedar Flat site. These configurations include a maximal configuration that includes baselines as long as 2 km, a compact configuration that offers a reasonable compromise between tight antenna packing and moderate sidelobe levels, and four intermediate configurations. Together the six configurations offer the astronomer choices in resolution of a factor of ∼2–2.5 between adjacent arrays. We refer to the configurations by the letters A (largest) through F (smallest). We have explored configurations using six 10.4m OVRO antennas and nine 6.1m BIMA antennas, and we defer consideration of the 3.5m SZA dishes.

2. The Configurations

The six configurations are shown in Figure 1, where shared stations are indicated by multiple symbols. The five A-E configurations are also shown together on a masked topographical map of the site in Figure 2, using the same symbols as in Figure 1. These five configurations are also shown individually on detailed topographical maps in Figures 3–7. The station positions for all arrays are listed in Table 1.

3. How Were the Configurations Generated?

The arrays were generated with the help of F. Boone's optimization code, subject to site constraints where appropriate. Boone's code optimizes for a gaussian-like *uv* density, using input constraints that specify the desired width of the gaussian and the size of the array. The optimization code ignores differences in elevation as a function of location on the site. We expect the elevation differences to yield relatively small perturbations to the solutions presented here, since the actual elevation differences are small in the case of the more compact arrays and since larger elevation differences have less of an impact for the larger arrays. This issue may be explored with an *a posteriori* analysis.

3.1. Practical Notes on Boone's Code

(1) In practice, the code optimizes better for a gaussian fit at large and intermediate *uv* distances and does not try to put antennas close together to generate (even relatively) short spacings. It was instead generally necessary to design the short spacings by hand. For the

compact configurations, it was not uncommon to get results with the shortest baselines 3 or more times larger than the desired minimum baselines.

(2) The inputs to Boone's program include a guess for a starting configuration which then is optimized. In practice, it is possible to generate different optimized arrays with very similar properties given different initial configurations.

(3) By running Boone's code iteratively, one can check to see how fast the code converges. In practice, one needs to run $\pm 3h$ tracks to get good results, and several (3-4) iterations to get convergent arrays.

(4) One of us (TTH) is currently running a version of Boone's code that does not "shake" the antennas loose from potential local optimizations, which is appropriate for the more compact arrays but which may not be optimal for the larger arrays. Since MCHW designed the A and B arrays, this does not affect these arrays.

3.2. Detailed Design Considerations

F array: The F array was generated with the goal of balancing very good *uv* coverage at short baselines (so as to be maximally sensitive to large structures on the sky) with very good beam quality (so as to have good imaging properties to those large structures). A sample placement of BIMA and OVRO dishes for F array is shown in Figure 8. At the heart of the F array is a set of five closely packed BIMA antennas that John Lugten designed as a subset of a concept for short-spacing *uv* data for the Allen Telescope Array (Lugten, ATA Memo in preparation). These five antennas work together to give complete coverage around the central "hole" in the *uv* plane. The remaining four BIMA antennas and six OVRO antennas were optimized using Boone's code, while holding the central five BIMA antennas fixed. After optimization, it was necessary to move two antenna positions slightly so as to avoid potential collisions with OVRO dishes. While the array was optimized for a declination of δ=15°, we then stretched the optimized array by 10% in the North-South direction to alleviate shadowing concerns and to get rounder beams for lower declination sources.

E array: We assumed that the E array, with $\sim 2''$ resolution at 230 GHz, will be the "workhorse" array at CARMA. As such, it was desirable for the E array to have as minimal spacings as well, though the *uv* coverage need not be as well sampled at short spacings as the F array was. The E array was therefore generated by fixing three BIMA antennas at close central pads from the F array. The other antennas were all free to move. As with the F array, the final, optimized E array was stretched by 10% in the North-South direction.

This array has a larger ratio of maximum to minimum baseline than do the other arrays (see §8) and pays a penalty of having a flatter than gaussian *uv* distribution (Figure 10) and therefore a central lobe with extended wings (Figure 9).

D array: The D array was optimized using Boone's code with a scaled version of John Lugten's 5-element subarray and letting the other 10 antennas freely move. We stretched the optimized array by 10% in the North-South direction and also shifted one of the antennas a bit so that it was possible to share two stations with the E array.

A and B arrays: We skip now to the A array, which was optimized using Boone's code, subject to the site constraints. The A array was a special case, in that the site constraints were most severe for this array. In particular, the highway Rte 168 that bifurcates the Cedar site posed a special practical challenge in the design of the A array. The four westernmost antennas are west of Rte 168. The B array was then optimized to be a maximal array on the east side of Rte 168 by fixing nine antennas to their A array positions and using Boone's code to optimize the remaining six antennas.

C array: Finally, the C array was optimized using Boone's code and fixing 8 antennas to their B positions and another two antennas to their D array positions.

4. Shared Stations

In all, 65 stations are needed to populate the six proposed arrays, given the assumption that there will not be a central concrete slab. As shown in Figure 1 and Table 1, the F array shares three pads with the E array. The E array shares two pads with the D array. The D array shares three pads with the C array. The C array shares eight pads with the B array. The B and A arrays share nine pads.

If we include a central large slab that covers most or all of the F array, then the number of reinforced stations may be substantially reduced. A $\sim$60m$\times$70m slab would be required to cover all of the F array; this slab would support 20 antennas and leave an additional 45 stations needed for the larger arrays. A smaller slab could instead be used to accommodate fewer of the compact antenna locations.

We note that for the compact arrays, a small perturbation of the antenna positions can lead to a dramatic change in the resultant *uv* coverage. For this reason, there tend to be fewer shared stations for the compact arrays and more shared stations for the larger arrays.

5. Beam Sizes and Sidelobes

Sample beam sizes and related parameters are listed in Table 2, for ν=230 GHz and declinations δ=30,0,-30°. The F array yields naturally-weighted beams of about 4.2″ at 230 GHz, down to 0.13″ beams available in A array. The beam elongations, listed in Table 3 for δ=0°, range from 1.07 to 1.17 for this declination.

The beams, which are shown in Figure 9, are generally well behaved, with near-in rms sidelobe levels of about 2–3% and peak near-in sidelobe levels of about 7% away from the equator. Figure 10 shows plots of the uv density as a function of radius for the different arrays.

6. Shadowing

In general, the shadowing properties of these configurations (Table 2) are excellent. Arrays A through D have no shadowing at any declination for 4-hour tracks. Even the most compact E and F arrays have no shadowing for declinations greater than $\delta = 0°$ for a 4-hour track. For $\delta = -10°$, only 5% of the E array visibilities and 9% of the F array visibilities are shadowed in a 4-hour track. By $\delta = -20°$, about 10% of the E array and 30% of the F array visibilities are shadowed. For the lowest declinations ($\delta = -30°$), 19% of the visibilities are shadowed in a 4-hour track for the E array and 54% of the visibilities are shadowed for the F array. It may be possible to alleviate the shadowing for these southernmost sources by adopting a different rotation of the current F array.

7. Scale Resolution Factors

The scale resolution factors (SRFs) between adjacent arrays are listed in Table 3. The SRFs among adjacent arrays range from 1.3 between the C and B arrays to 2.7 between the D and C arrays. These compare favorably with the current situation at BIMA, where the SRF is 2.1 between the BIMA D and C arrays, 2.8 between the BIMA C and B arrays, and 7.1 between the BIMA B and A arrays. These also compare well with the current situation at OVRO, where the SRF is 2 between the OVRO Compact and Low arrays and 3 between the OVRO Low and Low+High arrays.

8. Spatial Dynamic Range

The ratios of maximum to minimum projected baselines, which is a measure of the spatial dynamic range of a configuration, are also given in Table 3. For the most compact F array and for the most spread out A array, S_{max}/S_{min} is somewhat smaller than for the other arrays. These choices reflect the desire to have these arrays be most sensitive to short (F) or long (A) baselines. For the intermediate arrays, S_{max}/S_{min} is about 13. The exception is the E array, which has a larger spatial dynamic range of 21 in order to achieve the desired resolution while accommodating the shortest possible spacings.

9. Conclusions

We have presented a set of six configurations which are fitted to the Cedar Flat site. We discussed the overall method by which the configurations were generated as well as specific design considerations for the various arrays. We also discussed some basic properties of the arrays, including beam characteristics, shared stations, and shadowing.

Table 1. CARMA Stations

East (m)	North (m)	Up (m)	F	E	D	C	B	A
-1166.000	-156.000	0	...	...	...	...	...	X
-1108.000	883.000	0	...	...	...	...	...	X
-866.000	650.000	0	...	...	...	...	...	X
-823.000	78.000	0	...	...	...	...	...	X
-527.347	-1009.919	0	...	...	...	...	...	X
-443.059	-534.937	0	...	...	...	...	X	X
-395.419	229.525	0	...	...	...	X	X	X
-353.809	334.931	0	...	...	...	...	X	...
-310.626	-217.447	0	...	...	...	X	...	...
-306.880	-117.288	0	...	...	...	X	X	X
-262.300	888.265	0	...	...	...	...	...	X
-221.228	253.406	0	...	...	...	X	...	...
-171.641	-77.403	0	...	...	...	...	X	...
-159.830	89.454	0	...	...	...	X	...	...
-93.559	37.684	0	...	...	...	X	X	...
-93.281	608.442	0	...	...	...	...	X	X
-87.041	209.521	0	...	...	X	X	X	X
-76.544	-600.680	0	...	...	...	...	X	X
-75.798	-398.321	0	...	...	...	X	...	...
-52.138	280.038	0	...	...	X	...	...	...
-51.62	85.449	0	...	...	X	...	...	...
-46.157	158.117	0	...	...	X	...	...	...
-29.881	-3.521	0	...	...	X	X	...	...
-23.885	149.021	0	...	X	...	...	...	...
-14.159	318.403	0	...	...	X	...	...	...
-11.869	108.678	0	...	X	...	...	...	...
-9.164	-95.569	0	...	...	...	X	X	...
-5.194	91.6197	0	...	X	...	...	...	...
-3.968	181.461	0	...	...	X	...	...	...
-1.355	139.979	0	X	...	...	...	...	...
-0.568	123.125	0	X	...	...	...	...	...
4.234	190.792	0	...	X	...	...	...	...
4.827	142.665	0	...	X	X	...	...	...
5.371	58.5207	0	...	X	...	...	...	...
6.353	112.145	0	X	...	...	...	...	...
6.701	102.005	0	X	...	...	...	...	...
7.778	119.268	0	...	X	...	...	...	...

Table 1—Continued

East (m)	North (m)	Up (m)	F	E	D	C	B	A
9.808	77.2823	0	X	...	...	...	...	...
13.773	143.777	0	X	...	...	...	...	...
15.036	119.989	0	X	...	...	...	...	...
17.479	109.212	0	X	...	...	...	...	...
17.925	94.1464	0	X	...	...	...	...	...
22.527	116.32	0	X	X	...	...	...	...
23.000	168.255	0	...	...	X	...	...	...
24.938	79.719	0	...	X	X	...	...	...
27.575	109.212	0	X	X	...	...	...	...
30.018	119.989	0	X	X	...	...	...	...
36.03	132.833	0	X	...	...	...	...	...
37.224	98.626	0	X	...	...	...	...	...
40.608	96.351	0	...	X	...	...	...	...
40.900	-298.216	0	...	...	...	X	X	X
41.173	142.665	0	...	...	X	...	...	...
42.367	172.687	0	...	...	...	...	X	...
49.968	181.461	0	...	...	X	X	...	...
52.917	121.378	0	X	...	...	...	...	...
53.233	34.261	0	...	...	...	X	...	...
58.575	180.503	0	...	X	...	...	...	...
64.049	71.5623	0	...	X	...	...	...	...
91.713	120.54	0	...	X	...	...	...	...
102.621	16.420	0	...	...	...	...	X	...
103.03	109.627	0	...	...	X	...	...	...
131.762	229.825	0	...	...	X	...	...	...
149.01	176.509	0	...	...	X	...	...	...
217.410	-78.261	0	...	...	...	X	X	X
227.896	269.965	0	...	...	...	X	X	X

Table 2. Beam sizes, sensitivities, sidelobes, shadowing, and spatial dynamic ranges at ν=230 GHz for δ=30,0,-30°

Config	δ (°)	HA (hrs)	σ (mJy)	θ_{maj} x θ_{min} ($''$)	σ_{Tb} (mK)	Sidelobe rms[a] (%)	... max[a] (%)	... min[a] (%)	Nvis[b] (%)	uv min[c] (m)	uv max[c] (m)
A	30	-2,2,.01	0.23	0.15 x 0.12	295.4	2.9	7.1	-7.2	100	267.9	1981.2
	0	-2,2,.01	0.27	0.16 x 0.14	278.7	3.4	18.8	-7.3	100	195.3	1852.8
	-30	-2,2,.01	0.56	0.31 x 0.15	278.4	2.4	6.0	-6.9	100	99	1620
B	30	-2,2,.01	0.23	0.32 x 0.22	75.5	3.2	8.8	-6.7	100	111	1208.7
	0	-2,2,.01	0.27	0.31 x 0.27	74.6	3.3	12.2	-6.9	100	84	1118.7
	-30	-2,2,.01	0.56	0.55 x 0.32	73.6	2.2	6.0	-7.4	100	34.8	971.1
C	30	-2,2,.01	0.23	0.37 x 0.32	44.9	2.6	9.9	-6.6	100	69.9	734.7
	0	-2,2,.01	0.27	0.40 x 0.37	42.2	3.0	14.3	-6.8	100	54	726.9
	-30	-2,2,.01	0.56	0.83 x 0.37	42.2	2.3	5.5	-7.1	100	33.9	703.8
D	30	-2,2,.01	0.23	0.96 x 0.87	6.4	2.1	5.7	-6.4	100	27.3	322.2
	0	-2,2,.01	0.27	1.09 x 0.96	6.0	2.7	11.9	-7.0	100	21.9	281.1
	-30	-2,2,.01	0.56	2.17 x 0.99	6.0	2.1	8.3	-6.5	100	10.2	253.2
E	30	-2,2,.01	0.23	2.34 x 1.82	1.2	2.4	6.8	-6.3	100	7.5	133.5
	0	-2,2,.01	0.27	2.50 x 2.13	1.2	2.9	11.7	-6.8	100	6	129.3
	-30	-2,2,.01	0.63	4.40 x 2.18	1.5	2.7	7.2	-6.4	81	2.7	119.1
F	30	-2,2,.01	0.23	4.52 x 3.87	0.3	2.9	9.6	-6.4	100	7.5	66.6
	0	-2,2,.01	0.27	4.84 x 4.52	0.3	3.3	14.9	-7.0	100	6	61.8
	-30	-2,2,.01	0.83	7.81 x 3.91	0.6	4.2	15.6	-9.3	46	2.7	58.8

[a]Sidelobe rms, max, min measured over central ∼14 x 14 beamwidths

[b]Percentage of unshadowed visibilities for given hour angle range

[c]Projected minimum and maximum baselines

Table 3. Beam elongations, spatial dynamic ranges, and SRFs at ν=230 GHz and δ=0°

Config	θ_{maj} ($''$)	θ_{min} ($''$)	$\theta_{maj}/\theta_{min}$	S_{max}/S_{min}[a]	SRF[b]
A	0.16	0.14	1.14	9.5	
B	0.31	0.27	1.15	13.3	B/A = 1.9
C	0.40	0.37	1.08	13.5	C/B = 1.3
D	1.09	0.96	1.14	12.8	D/C = 2.7
E	2.50	2.13	1.17	21.6	E/D = 2.3
F	4.84	4.52	1.07	10.3	F/E = 2.0

[a]Ratio of maximum projected baseline to minimum projected baseline

[b]Scale resolution factor between adjacent arrays

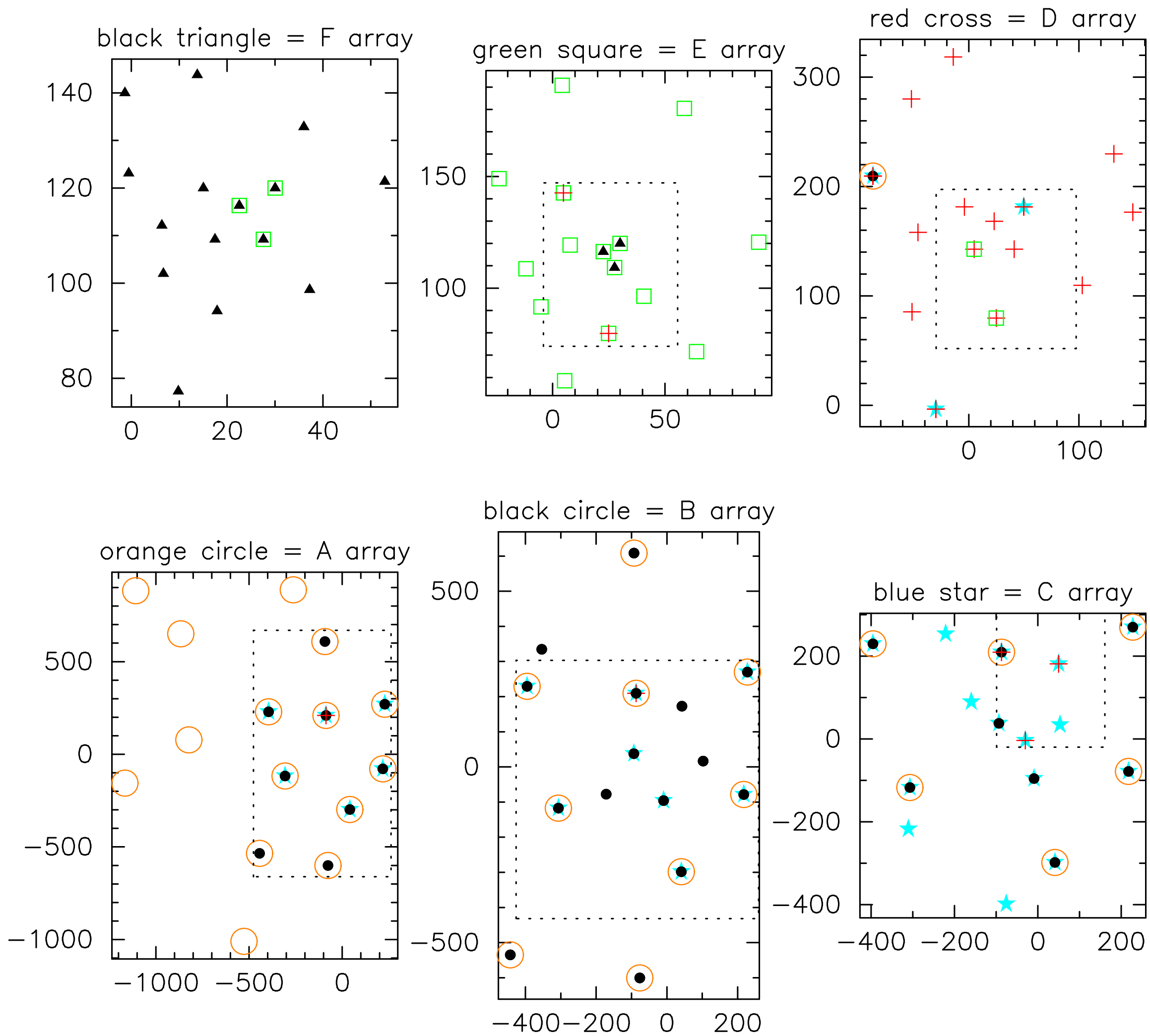

Fig. 1.— CARMA configurations. The abscissa (ordinate) is east (north) coordinates in meters. The dotted rectangles represent the outline of the next-smallest configuration. Shared stations are indicated by multiple symbols.

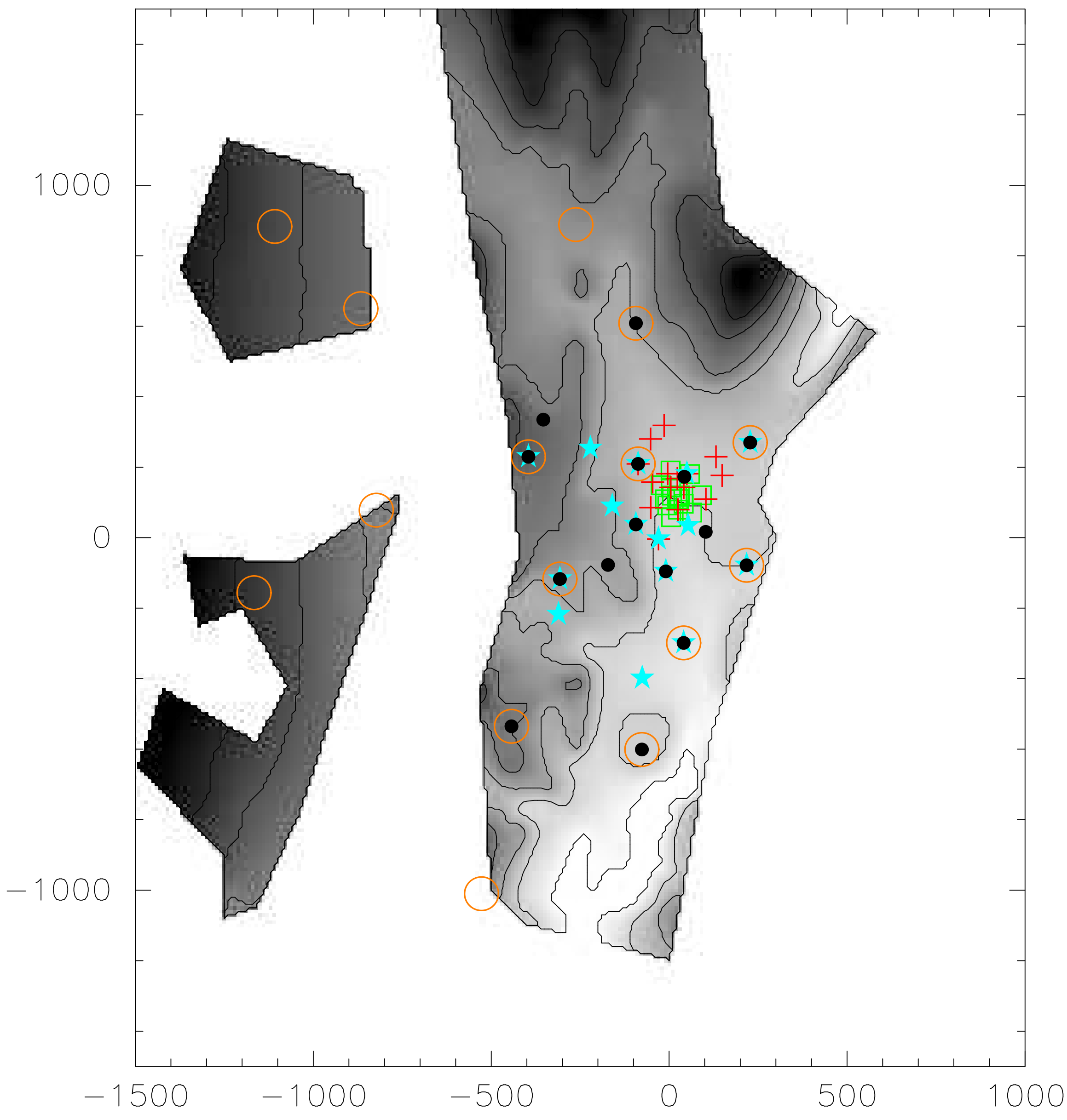

Fig. 2.— A, B, C, D, and E configurations overlaid on the site, shown with a mask used to exclude Rte. 168 and difficult terrain. Symbols are as in Figure 1. The abscissa (ordinate) is east (north) coordinates in meters.

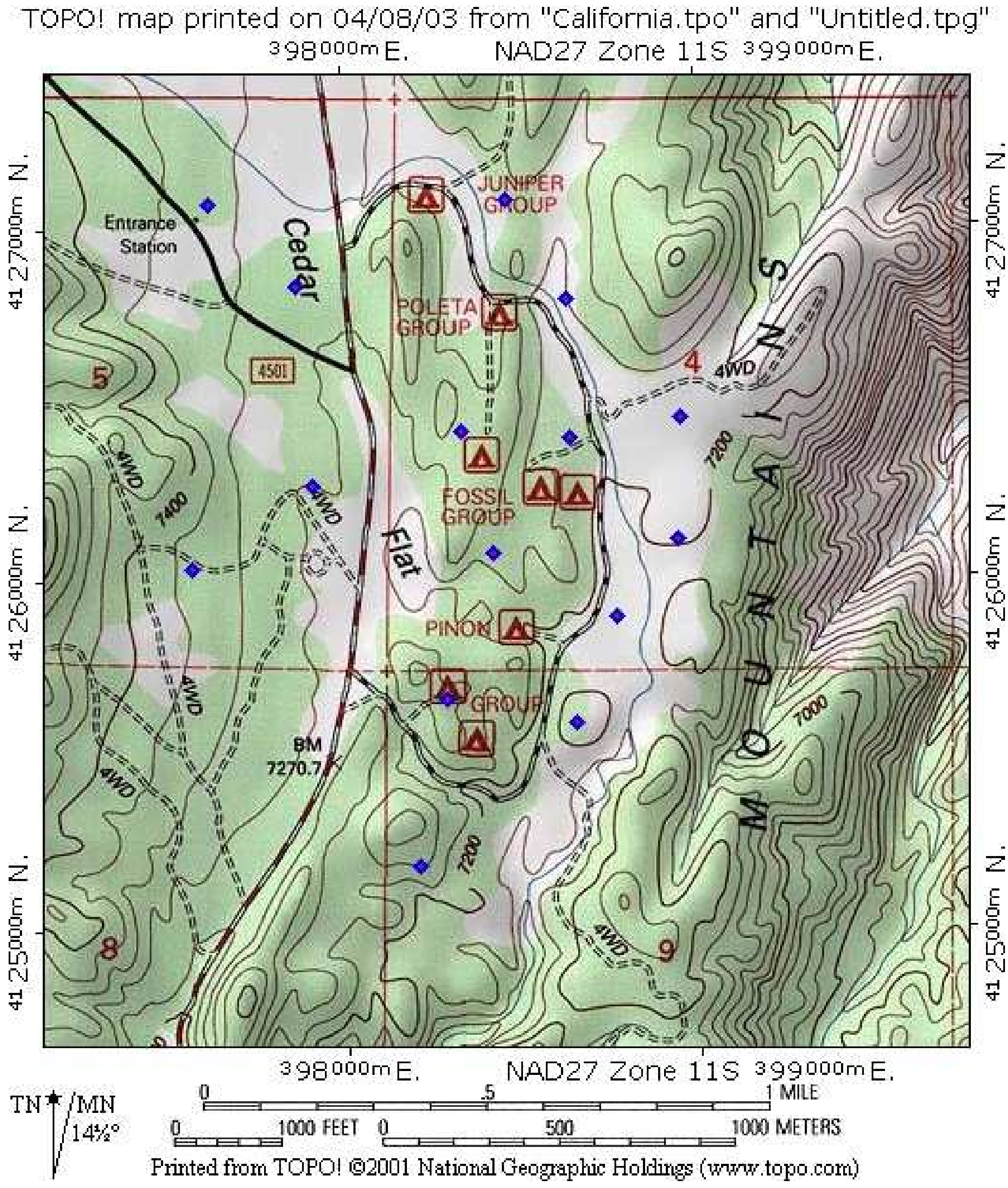

Fig. 3.— A array stations, shown as blue diamonds, overlaid on a topographical map of the Cedar site.

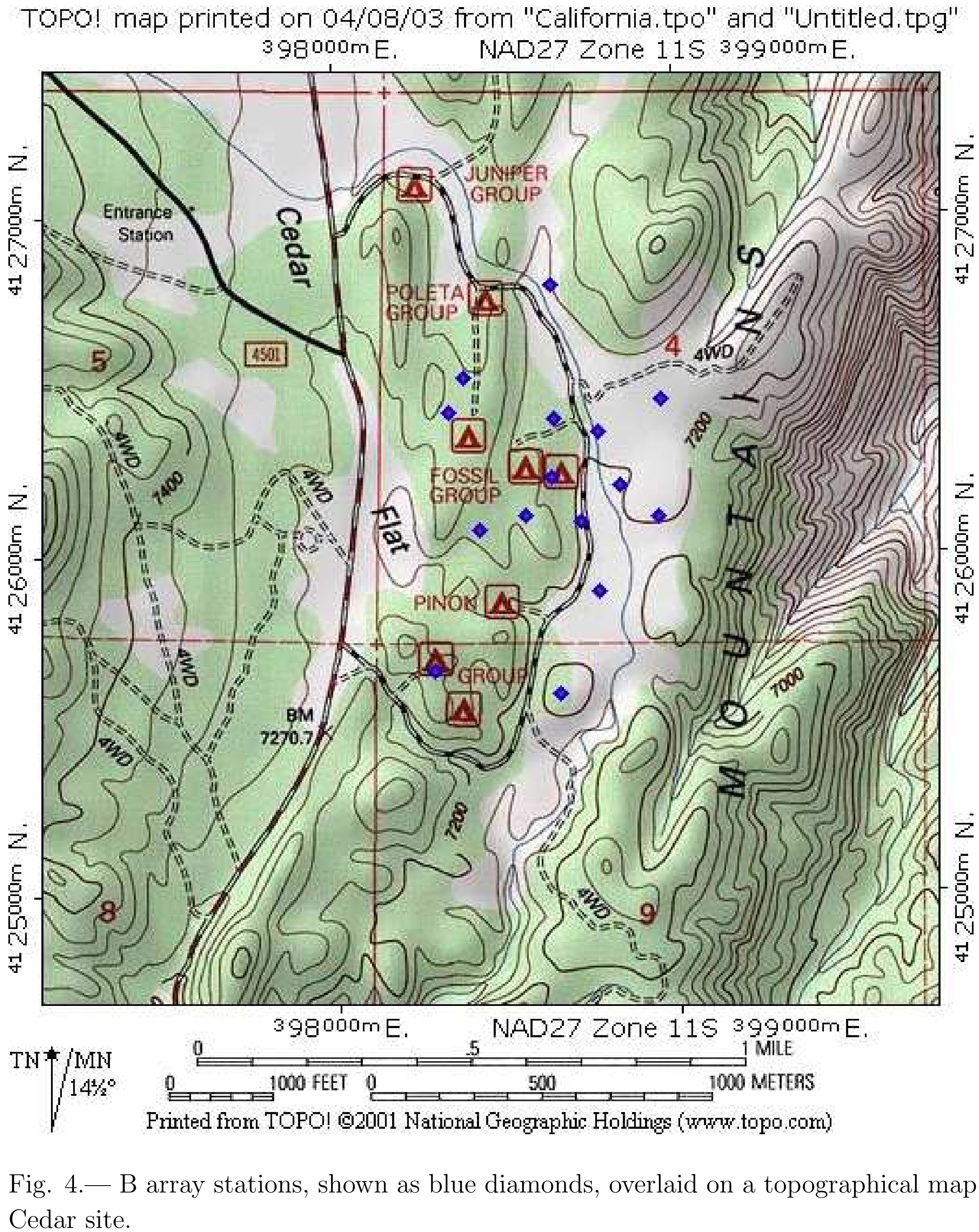

Fig. 4.— B array stations, shown as blue diamonds, overlaid on a topographical map of the Cedar site.

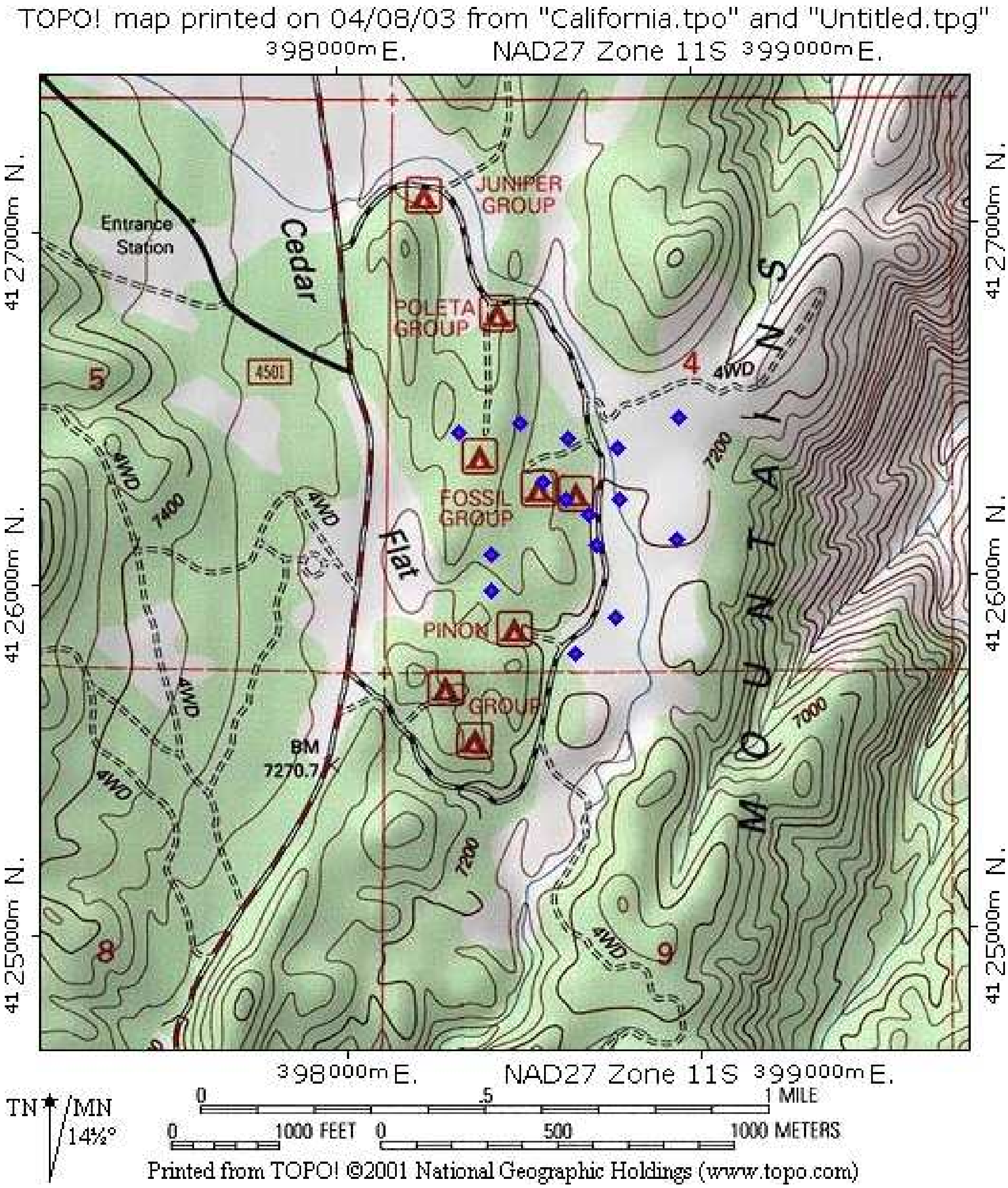

Fig. 5.— C array stations, shown as blue diamonds, overlaid on a topographical map of the Cedar site.

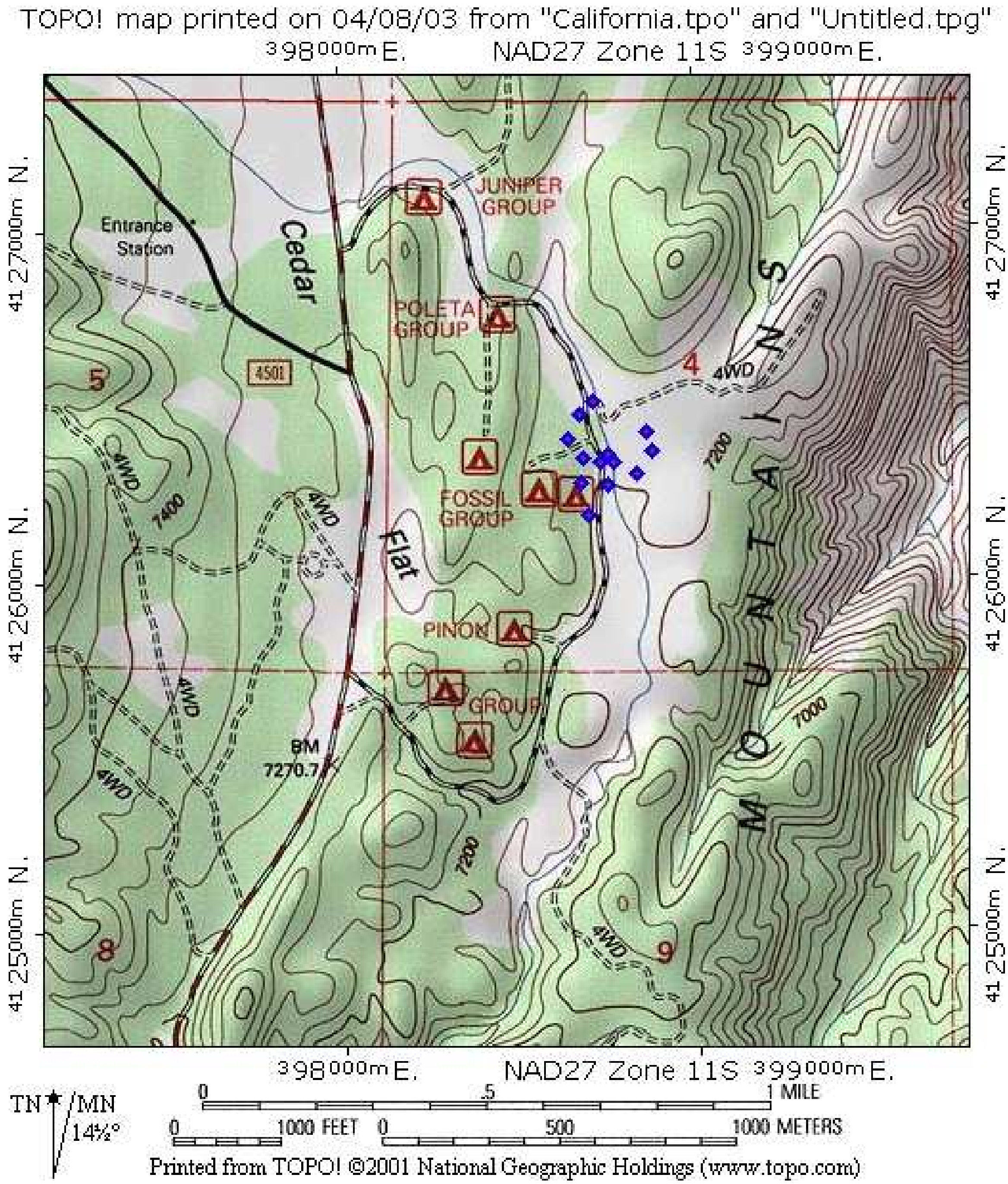

Fig. 6.— D array stations, shown as blue diamonds, overlaid on a topographical map of the Cedar site. (At the resolution of the map, some of the stations are blended together.)

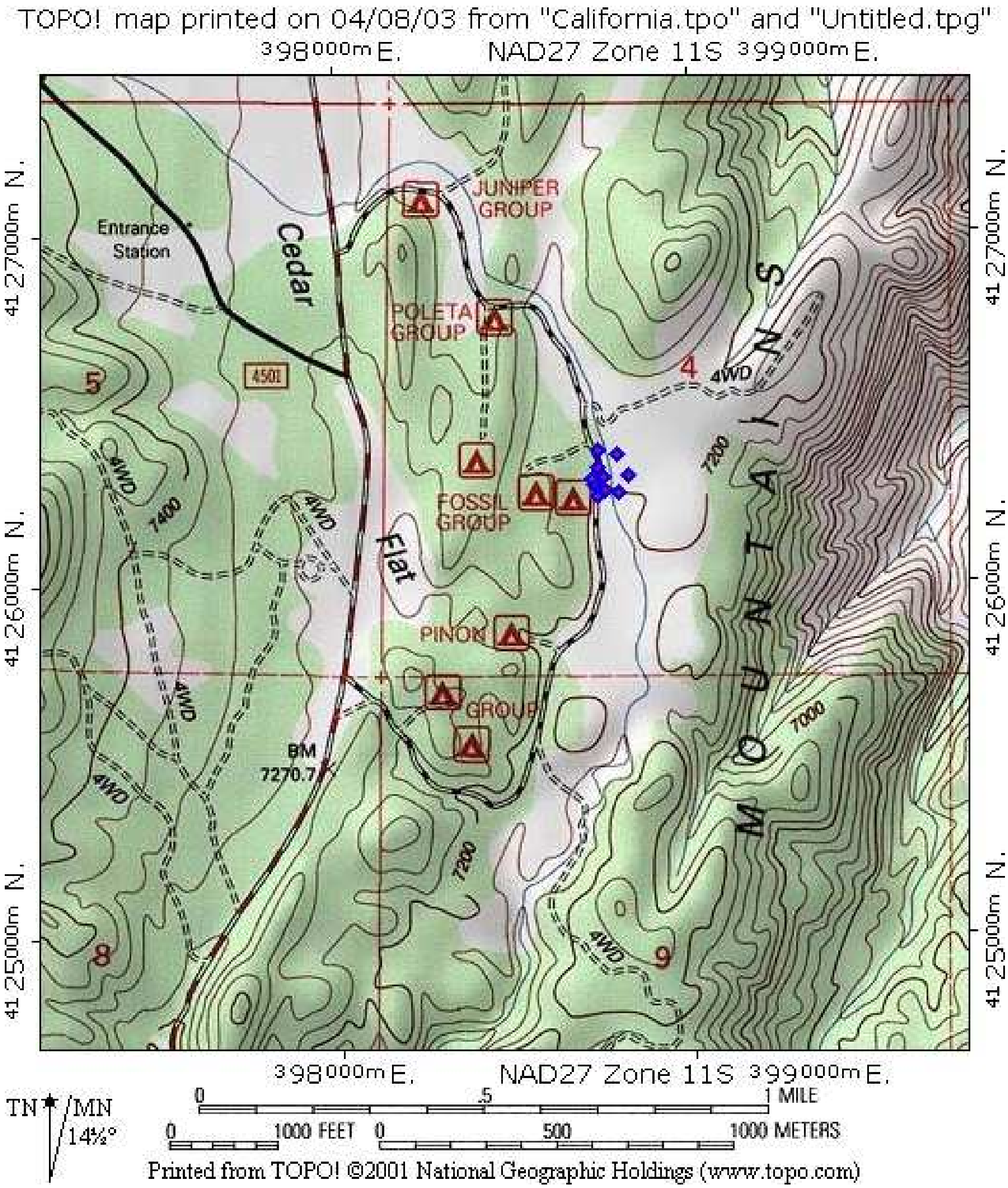

Fig. 7.— E array stations, shown as blue diamonds, overlaid on a topographical map of the Cedar site. (At the resolution of the map, some of the stations are blended together.)

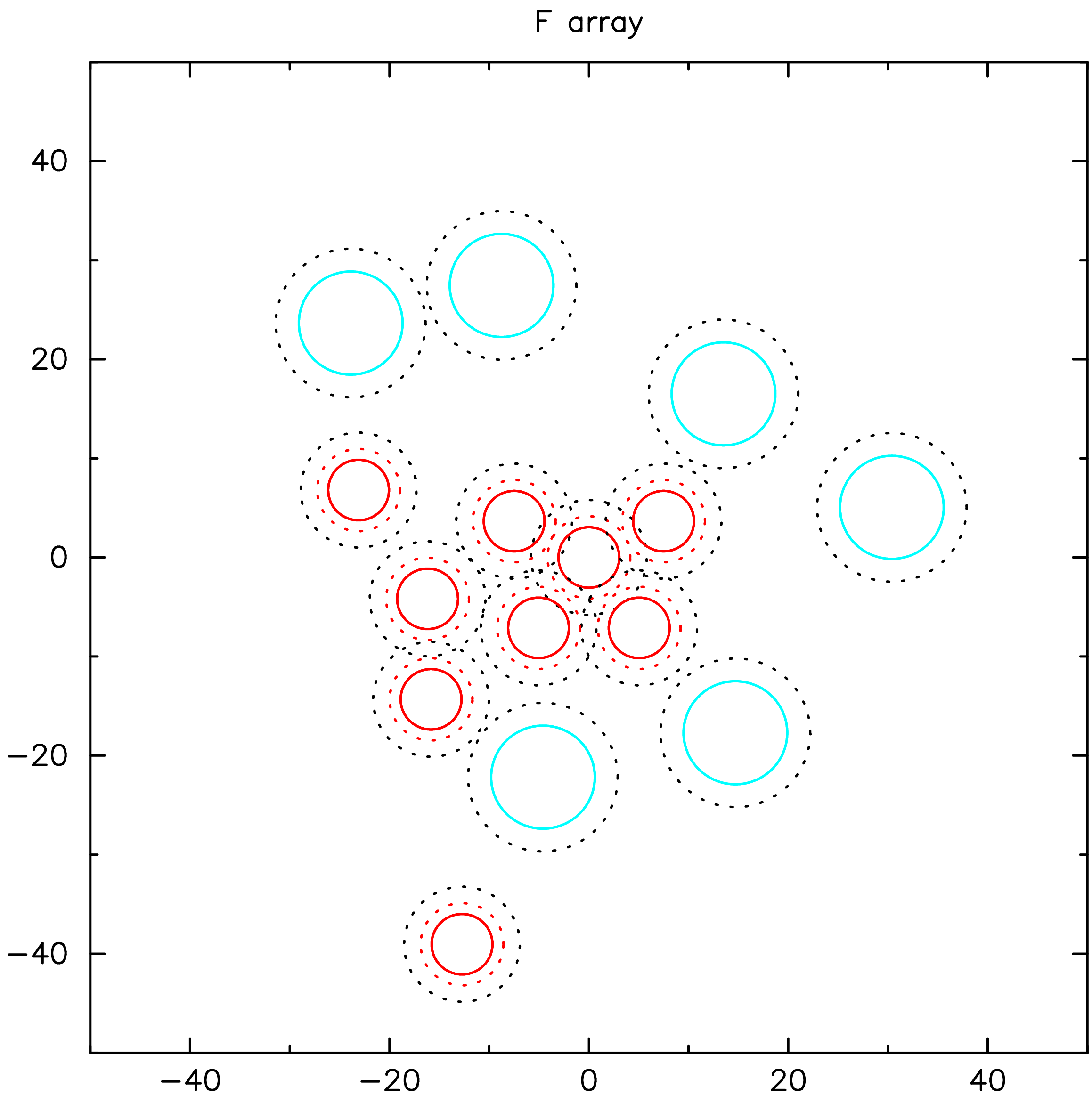

Fig. 8.— CARMA F array, shown with a sample placement of the two kinds of antennas. The abscissa (ordinate) is east (north) coordinates in meters. The 10.4m diameter of the OVRO antennas are shown as blue circles; the black dashed circles around the OVRO dishes are 15m in diameter, which is the collision-avoidance limit. The 6.1m diameter BIMA dishes are shown as solid red circles. The dashed red circles show the 8.3m closest-approach limit between BIMA dishes, which require collision avoidance hardware/software to implement (as is currently done at BIMA). The dashed black circles represent the 11.6m collision-avoidance limit for the BIMA dishes.

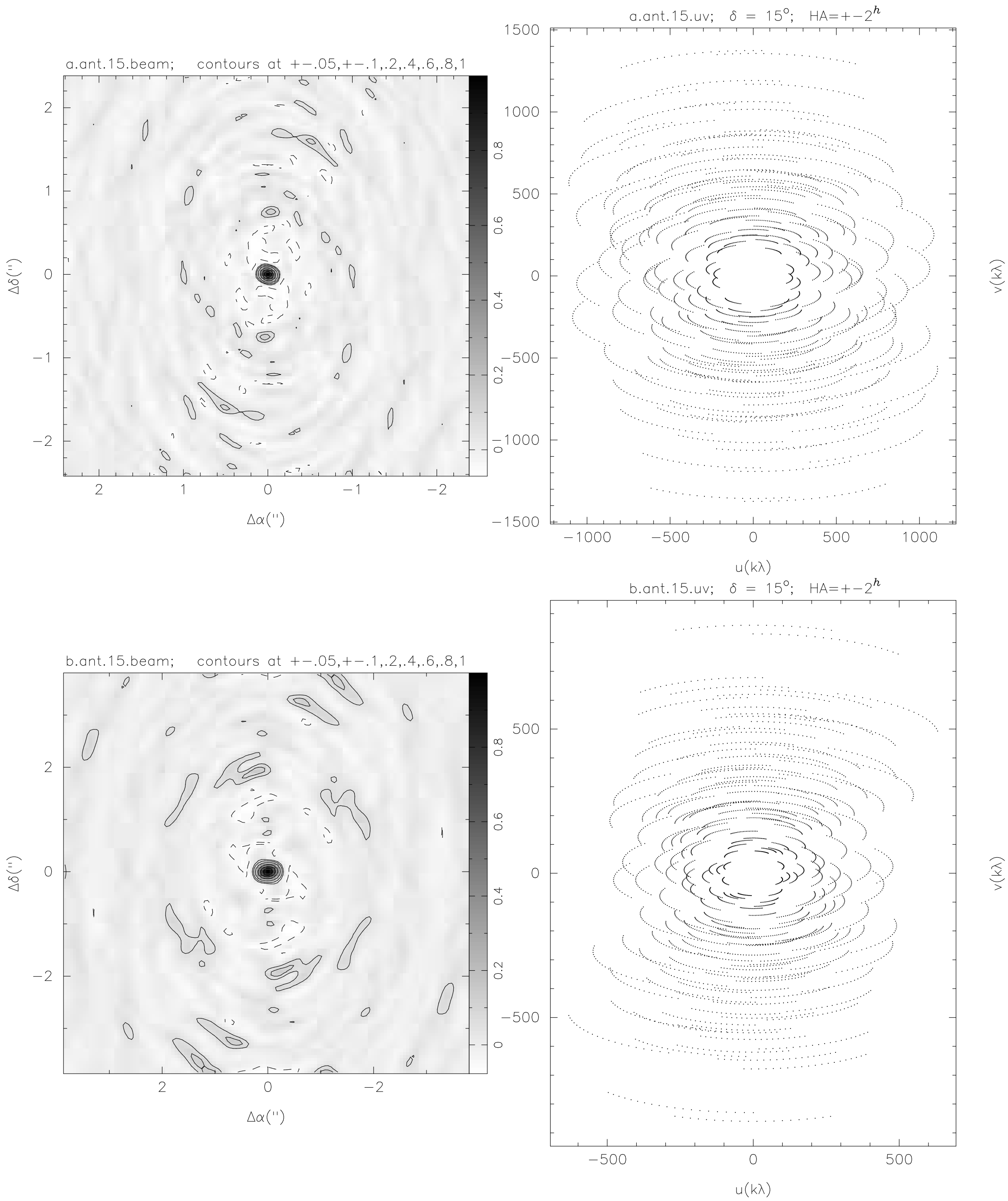

Fig. 9.— Naturally weighted beams (left column) and uv coverages (right column) for ±2-hour tracks run at ν=230 GHz and δ=15°, for A array (top row) and B array (bottom row). Contours are listed at the top of the beam plots.

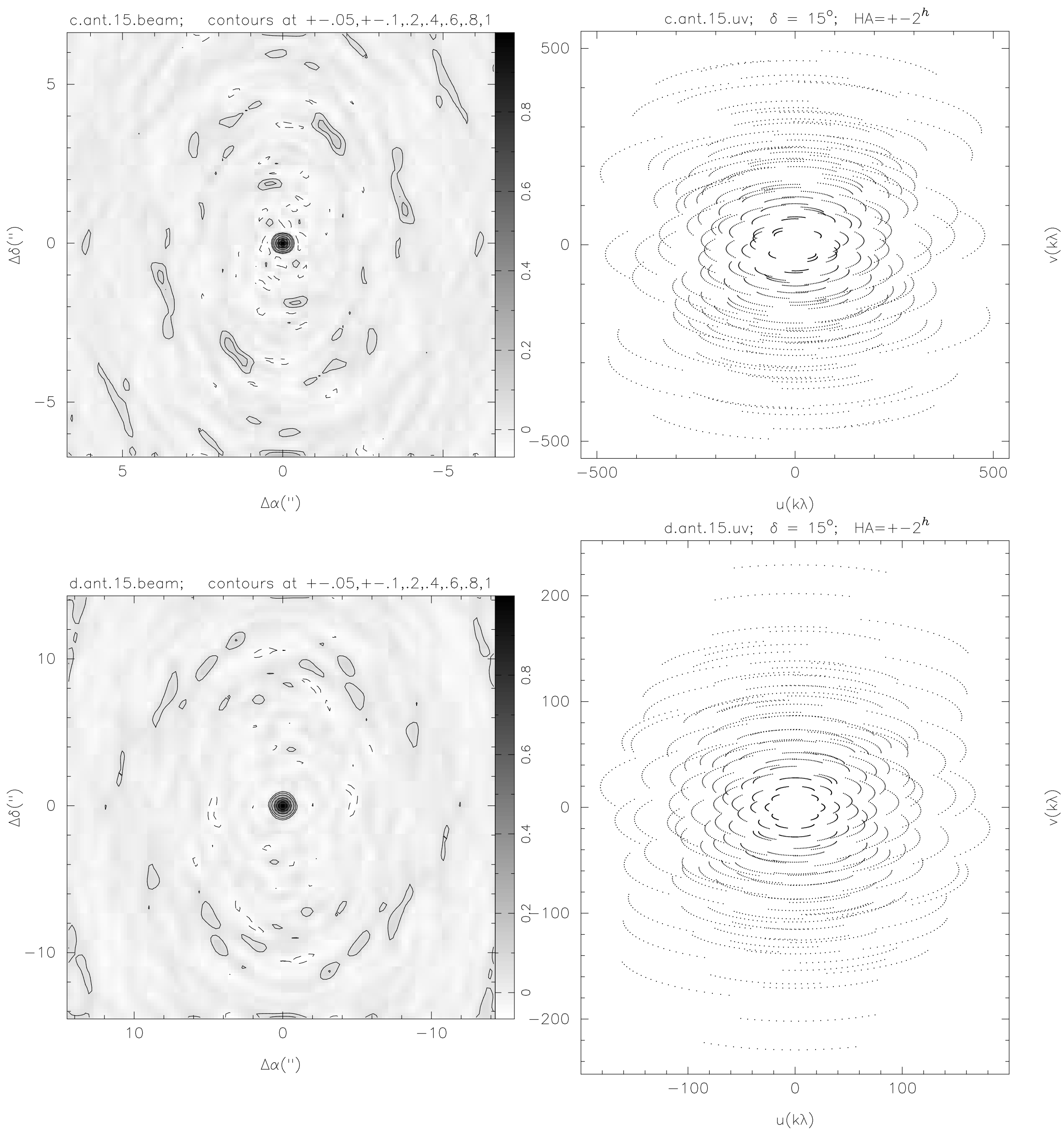

Fig. 9–cont.— Naturally weighted beams (left column) and *uv* coverages (right column) for ±2-hour tracks run at ν=230 GHz and δ=15°, for C array (top row) and D array (bottom row). Contours are listed at the top of the beam plots.

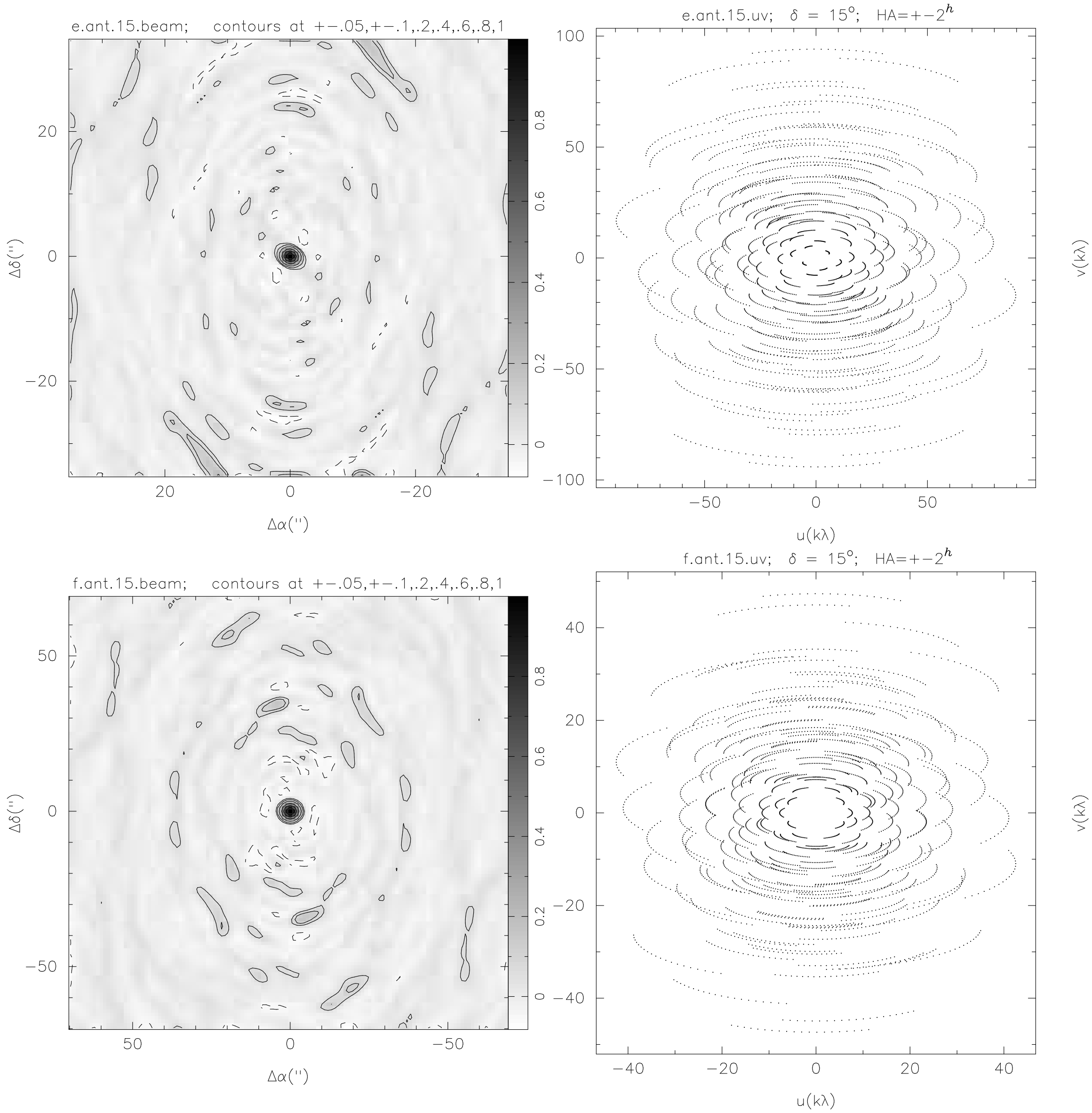

Fig. 9–cont.— Naturally weighted beams (left column) and *uv* coverages (right column) for $\pm$2-hour tracks run at ν=230 GHz and δ=15°, for E array (top row) and F array (bottom row). Contours are listed at the top of the beam plots.

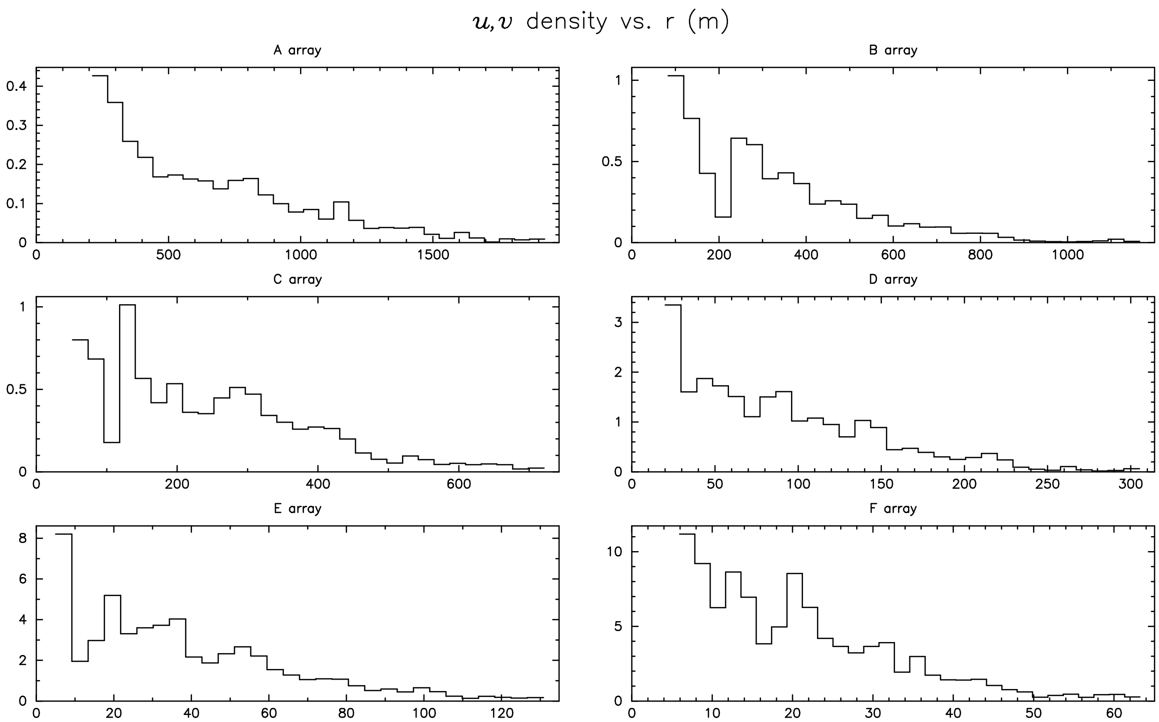

Fig. 10.— Histograms of uv density as a function of radius for the different arrays.